Micro-Raman spectroscopy on YBCO films during heat treatment

2002 Supercond. Sci. Technol. 15 1606

(http://iopscience.iop.org/0953-2048/15/11/321)

INSTITUTE OF PHYSICS PUBLISHING SUPERCONDUCTOR SCIENCE AND TECHNOLOGY
Supercond. Sci. Technol. **15** (2002) 1606–1609 PII: S0953-2048(02)32044-X

Micro-Raman spectroscopy on YBCO films during heat treatment

C Camerlingo[1], I Delfino[2] and M Lepore[3]

[1] Istituto di Cibernetica 'E Caianiello' del Consiglio Nazionale delle Ricerche, Via Campi Flegrei 34, 80078 Pozzuoli, Italy
[2] Istituto Nazionale di Fisica della Materia, UdR Napoli, Napoli, Italy
[3] Dipartimento di Medicina Sperimentale, Seconda Università di Napoli, Napoli, Italy

Received 19 December 2001, in final form 24 September 2002
Published 18 October 2002
Online at stacks.iop.org/SUST/15/1606

Abstract
The oxygen content and the local oxygen arrangement of $YBa_2Cu_3O_{7-x}$ (YBCO) thin films grown on $NdGaO_3$ substrates have been monitored by micro-Raman spectroscopy. The analysis was performed during the heat treatment of the sample in air, with temperatures T_a ranging between 20–300 °C. At $T_a < 220$ °C, the superconductivity of the samples was preserved, the critical temperature T_c being in the range of 86–90.7 K. At higher heating temperatures, the zero voltage state was suppressed due to the loss of oxygen. Evidence of fully oxygenated phase domains was nevertheless observed, proving the existence of a multiphase structure. The dramatic changes in the electrical characteristics are thus attributed to grain boundary region de-oxygenation, revealing the important role of planar-type defects on the transport properties of the films.

1. Introduction

The role of structural defects on the magnetic and transport properties of high-T_c superconductors is of great relevance in films, due to the critical influence they have on the dynamics of the quantized magnetic flux lines (vortices) which can penetrate the sample when it is placed in an external magnetic field. These effects increase the final noise figure of devices based on high-T_c superconductor films and limit the great potential of microelectronics and ultra-sensitive device applications, such as for instance bio-magnetic field sensors. Recently, it has been pointed out that the correlated columnar defects, which intrinsically occur in YBCO films grown on $SrTiO_3$ substrates, have a significant influence on magnetic behaviour [1, 2]. $NdGaO_3$ substrates also allow the fabrication of YBCO films of high quality, with regard to the superconducting properties and surface morphology. In contrast to the $SrTiO_3$ case, planar defects are expected to be induced in YBCO films grown on $NdGaO_3$, due to the formation of reciprocally twinned grains. Raman spectroscopy provides a unique tool for detecting out-of-phase and structural disorder micro-domains, not otherwise visible in conventional x-ray diffractometry [3].

In this paper, we report on micro-Raman measurements performed on YBCO thin films deposited on $NdGaO_3$ substrates. The sample was heated slowly in air in order to study the structural degradation and oxygen diffusion processes. The evolution of the Raman response was recorded using an *in situ* micro-Raman set-up. The heating temperature was increased in steps from 20 °C up to 300 °C. After each step, consisting of two hours of measurements at a constant temperature, the critical temperature T_c was evaluated by the dependence on the temperature of the electrical resistance.

2. Experimental details

The films have been fabricated by inverted cylindrical dc magnetron sputtering. The deposition process was performed in a 4:3 atmosphere of Ar and O_2, at a pressure of 700 mTorr. The material was sputtered from a stoichiometric target on the substrate heated at a temperature of 810 °C. In order to improve the spatial thermal homogeneity, a back-coating of 500 nm of gold was previously deposited on the bottom face of the substrate. Before deposition, the substrate surface was cleaned for 30 min by a process of soft etching, using fast atom bombardment (FAB) in an oxygen atmosphere. During this treatment the sample was heated at 600 °C. One hour of annealing at 780 °C at a pressure of 1 Torr of oxygen was thus performed before the power on the magnetron plasma.

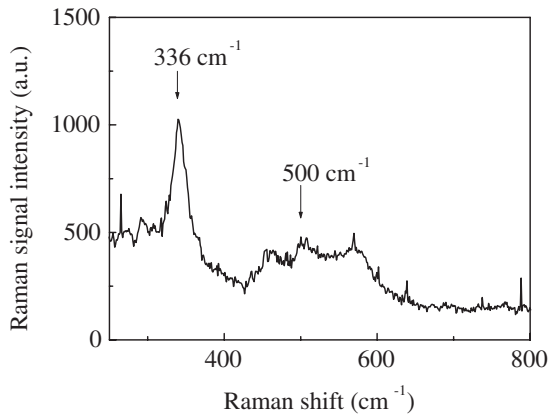

Figure 1. Micro-Raman spectrum of YBCO film growth on $NdGaO_3$ substrate.

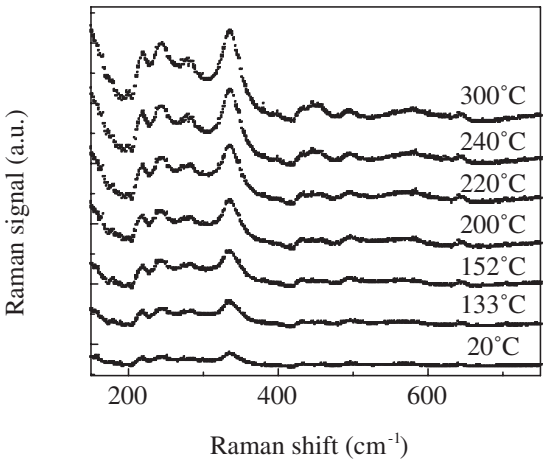

Figure 2. Micro-Raman spectra of a film of YBCO during 2 h of heat treatment. The spectra are measured on the same sample at different temperatures: $T_a = 20$, 133, 152, 200, 220, 240 and 300 °C. The curves are arbitrarily shifted along the vertical axis.

The 180 nm thick film considered here was *c*-axis oriented normal to the film surface. A superconductivity critical temperature, $T_c = 90.7$ K, was evaluated before heat treatment from the electrical resistance dependence on temperature. A bias current density lower than 1 μA cm^{-2} has been used in a four-contact configuration, using wedge-bonded Al/Si wiring. The measurements were made in a closed cycle refrigerator system. The micro-Raman response to a He–Ne laser light excitation, with wavelength $\lambda = 638$ nm, was collected by a Jobin-Yvon TriAx 180 monochromator, equipped with a liquid nitrogen cooled CCD detector.

The maximum laser beam power was 17 mW; the actual power dissipated on the sample was significantly attenuated with respect to this value, because the laser was connected to the detection apparatus through an optical fibre. A long work distance optical objective 20× was used in the backscattering configuration to focus incoming laser light on the sample and to collect the scattered signal. The laser spot diameter was about 10 μm. The excitation area was large enough to include a large number of crystalline grains constituting the YBCO films. The average grain size was, in fact, of the order of a few tens of nanometres [2]. The Raman spectrum characteristics did not depend on the acquisition position, inside the sample surface area of 5 × 5 mm^2. Furthermore, the measurements were stable and repeatable, suggesting that the used laser power did not significantly heat the sample during the experiment. The absence of significant laser-induced heating effects was also tested by considering the anti-Stokes–Stokes intensity ratio of a high intensity vibration. The sample was attached by silver paint on to an electrical heater at a distance of about 20 mm from the objective. Micro-Raman spectroscopy was performed during the heat treatment of the sample, for temperatures ranging between 20–300 °C. The acquisition time was 300 s. Each spectrum was measured twice, in order to eliminate cosmic radiation spikes.

3. Experimental results

Figure 1 shows the micro-Raman spectrum of the YBCO film before the heat treatment, clearly exhibiting the peaks positioned at energy shifts 336 cm^{-1} and ∼500 cm^{-1}. These two peaks concern, respectively, the vibration modes of oxygen of the CuO_2 planes (O2–O3 out-of-phase) and into apical sites (O4) of orthorhombic $YBa_2Cu_3O_{7-x}$. Their positions and their reciprocal intensity ratio are consistent with a well-oriented *c*-axis crystal orientation and a close optimal oxygen doping ($x \approx 0.06$ in the $YBa_2Cu_3O_{7-x}$ formula) [3, 4]. The YBCO film has been progressively annealed at increasing values of temperature of 133, 152, 200, 220, 240 and 300 °C. Starting from room temperature (20 °C) the sample temperature was slowly increased to each of the above listed values and kept constant for 2 h. During this time, the Raman spectrum was measured every 15 min. The spectra measured during each treatment step did not differ significantly each from each other, indicating that the structural changes occur in a short time with respect to the acquisition rate. The data accumulated during each step are reported in figure 2 and compared with those measured at room temperature (see figure 1). The curves are shifted along the vertical axis arbitrarily, and refer to increasing temperatures from the bottom to the top of the figure. For an annealing temperature larger than 150 °C, the temperature dependence of the electrical resistance has been measured after each heating process. The results are reported in figure 3, and compared with the dependence before treatment. The data are normalized to the value of the resistance at $T = 100$ K. The superconducting properties degrade sharply for an annealing temperature T_a larger than 200 °C, resulting in a semiconductor behaviour after the $T_a = 300$ °C heat treatment.

In order to correlate the observed electrical figure to the results of the Raman spectroscopy, we have analysed the spectra in the region around the $\nu_{O4} = 500$ cm^{-1} energy mode. As $NdGaO_3$ has some active modes in such a region, the Raman experimental curves have been deconvoluted in Lorentzian functions, and peaks attributed to the signal due to the substrate were subtracted (see figure 4). This procedure allows us to detect three main modes, with peak energy shifts ν_1, ν_2 and ν_3, standing in the ranges of 428–431 cm^{-1}, 489–498 cm^{-1} and 578–600 cm^{-1}, respectively. The estimated values of ν_i and their I_i intensity normalized to that of the 336 cm^{-1} peak (out-of-phase *c*-axis vibration of the O2–O3 oxygen atoms in the CuO_2 planes) are reported in table 1.

Table 1. Dependence on the heat treatment temperature T_a of the critical temperature T_c, of the width ΔT_c of the resistive transition, and of the positions ν_i and intensity I_i of the three Raman peaks occurring in the energy shift range of 425–600 cm^{-1}. The intensity values are normalized to the intensity of the peak occurring at $\nu = 336$ cm^{-1}.

T_a	T_c	ΔT_c	ν_1 (cm^{-1})	I_1	ν_2 (cm^{-1})	I_2	ν_3 (cm^{-1})	I_3
20°	90.7 K	1.0 K	431.2 ± 0.2	0.20	497.7 ± 0.5	0.26	577.7 ± 0.8	0.11
133°	–	–	429.9 ± 0.5	0.18	495.0 ± 0.5	0.24	586.3 ± 1.0	0.05
152°	89.4 K	1.4 K	429.8 ± 0.2	0.26	493.7 ± 0.5	0.22	586.1 ± 0.6	0.07
200°	88.2 K	4.0 K	427.9 ± 0.5	0.17	492.1 ± 0.6	0.24	590.1 ± 2.4	0.26
220°	86.0 K	7.0 K	–	–	484.6 ± 0.3	0.20	597 ± 2	0.76
240°	17.0 K	15.0 K	428.3 ± 0.3	0.07	489.2 ± 0.3	0.20	>600	–
300°	–	–	432.8 ± 0.3	0.05	488.7 ± 1.8	0.26	>600	–

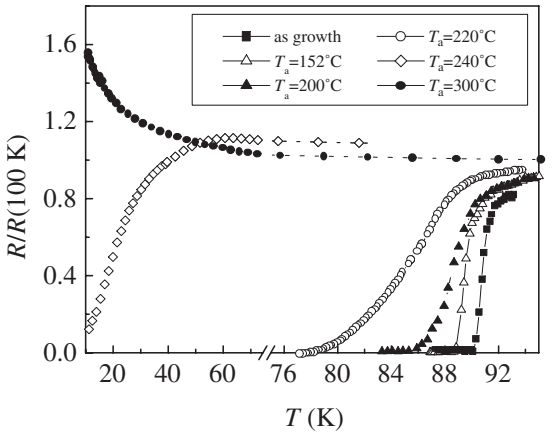

Figure 3. Temperature dependence of the electrical resistance of the YBCO film. Curves refer to the sample as-grown (■) and after heat treatments at temperatures $T_a = 152$ °C (△), 200 °C (▲), 220 °C (○), 240 °C (◇), and 300 °C (●). The resistance values are normalized to the value of resistance at $T = 100$ K.

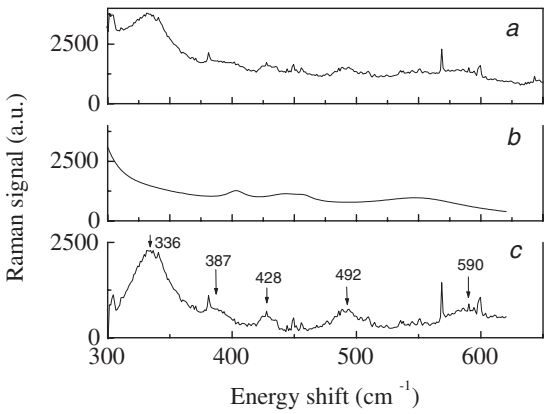

Figure 4. Experimental micro-Raman spectrum resulting from the accumulation of eight acquisition runs of the YBCO film on the $NdGaO_3$ substrate during heat treatment at $T_a = 200$ °C. The measured data (*a*) were deconvoluted in Lorentzian functions, and the peaks due to the Raman response of the $NdGaO_3$ substrate, the convolution of which is reported in (*b*), were subtracted. The remaining Lorentzian components, attributed to the YBCO film Raman response signal, were convoluted and curve (*c*) was obtained.

The ν_2 mode is attributed to the vibration of oxygen O4 in apical sites of orthorhombic phase of YBCO (ν_{O4} mode). This value is related to the oxygen content of $YBa_2Cu_3O_{7-x}$ by the empirical relation [5]

$$x = 0.025\nu_{O4} - 11.57. \qquad (1)$$

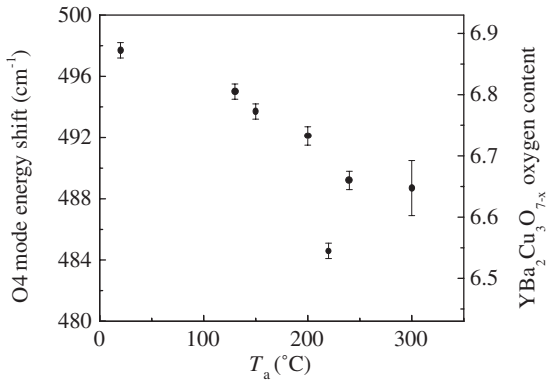

Figure 5. Experimental energy shift position of the apical oxygen mode of the YBCO film during heat treatments. On the *x*-axis we report the temperatures T_a at which the treatments were performed.

Figure 5 shows the dependence on T_a of the experimental evaluated value of ν_{O4} (left axis) and the corresponding value of $(7 - x)$ in $YBa_2Cu_3O_{7-x}$ calculated by equation (1) (right axis). With an increase in the annealing temperature T_a, the energy shift of the ν_{O4} mode decreases from the initial value of 498 cm^{-1} to about 484 cm^{-1} at $T_a = 220$ °C, after which it increases reaching a value of about 489 cm^{-1}. In spite of the significant reduction of T_c exhibited after sample treatment at $T_a > 200$ °C, the oxygen content inferred by Raman analysis is not low enough to justify the presence of a pure ortho-II phase, which occurs at $x \approx 0.53$–0.55. A multiphase superconducting region should be envisaged, in which high-T_c ortho-I phase ($x > 0.5$), ortho-II phase ($0.35 < x < 0.47$) and ordered tetragonal phase ($x < 0.8$) domains coexist on an atomic scale [6].

In this framework, the change of apical oxygen mode position in the spectrum results from the superposition of three different bands centred at ∼486, 493 and 503 cm^{-1}, and from their oxygen-dependent relative intensities.

The rapid decrease of the ν_{O4} value at the annealing temperature $T_a = 220$ °C is associated with a consistent loss of oxygen and with the formation of tetragonal phase regions. These regions are argued to be confined to the intergrain parts of the films, because the transition temperature remains relatively high ($T_c = 86.0$ K). The annealing mainly decreases the coupling between well-oxygenated superconducting grains.

With an increase of T_a, the loss of oxygen becomes stronger, the intergrain region becomes larger and the coupling between grains becomes weaker, resulting in the very low T_c

value and finally in the semiconductor behaviour observed. The intensity of the 486 cm^{-1} mode is expected to decrease for the pure tetragonal phase ($x = 1$) allowing the detection of the 493 cm^{-1} component, assigned to ortho-II phase domains. This interpretation is consistent with the T_a dependence of vibration modes labelled ν_1 and ν_3 (see table 1). The ν_1 mode can be attributed to in-phase vibrations of oxygen in the CuO_2 planes (O2–O3 in-phase). The energy shift of this mode is expected to change from 420 cm^{-1}, for optimal doping, to about 452 cm^{-1} for an oxygen-deficient sample ($x > 0.7$) [6]. The low experimental value of $\nu_1 \approx 430$ cm^{-1}, substantially constant with T_a, indicates the presence of optimal oxygenated phase domains also at the largest value of heating temperatures, even if the decrease of the peak intensity at $T_a > 220$ °C reflects a large diminution of their extension. An eventual additional peak originated by the poor oxygenated phase is hidden by the substrate Raman active mode located at 451 cm^{-1}. The ν_3 mode is typically present in Raman spectra of oxygen-deficient YBCO crystal [6], and has been observed in heated YBCO samples both in single-crystal [7] and in poly-crystal specimens [8]. Even if the origin of such a vibration mode is still unclear, it is generally accepted that it is the consequence of the presence of defects and oxygen vacancies in the CuO chains, which break the crystal inversion symmetry and make some infrared modes Raman active. In the case of YBCO, the infrared active modes are localized at 585 and 640 cm^{-1} [8]. The energy shift and the intensity of the Raman signal measured for this ν_3 mode increase with T_a. This feature is consistent with the results of measurements carried out by Burns *et al* on heated fully-oxygenated YBCO single-crystal samples [7]. In a subsequent paper, the same authors report that in YBCO single crystals with different oxygen contents, the ∼600 cm^{-1} peak appears in low oxygen content samples ($x > 0.7$) replacing in the spectrum the ν_{O4} mode peak [9]. The presence in the spectra of both ν_{O4} and ν_3 modes is thus a signature of the multiphase region. For $T_a > 220$ °C, the ortho-II phase domains become prevalent ($\nu_{O4} \sim 493$ cm^{-1}). The abrupt depression of the superconducting properties at $T_a > 220$ °C indicates that the poor oxygen phase domains are localized at the intergrain regions, where conditions for chain break are more probable. After the described treatments, the sample was kept at room temperature in a dry atmosphere. The Raman spectroscopy of the samples, performed at room temperature some days after, shows that some adjustment in the ordering of oxygen occur. Even if the general shape of the Raman spectrum remains qualitatively the same, the energy shift position of the peak attributed to the ν_{O4} mode increases, reaching values of 494.6 cm^{-1} after four days and 493.4 after fifteen days. This is attributed to an ordering process due to the diffusion of oxygen along large distances, which improve the perfection of the ortho-II phase domains. In a recent paper, Straube *et al* [10] have observed a similar ordering process in ortho-II phase YBCO single crystal, with a time constant estimated in 3.7 days for the recovery of the crystalline structure after heat treatments.

4. Conclusions

The changes induced by temperature on the spectral characteristics of YBCO film growth on $NdGaO_3$ substrates were experimentally investigated for temperature T_a ranging between 20–300 °C. The superconducting transition temperature is found to depend not only on the total oxygen concentration but also on local order. A multi-phase region, where ortho-I, ortho-II and tetragonal phase domains coexist, seems to give an appropriate picture of observed behaviour. After the heat treatment at $T_a = 300$ °C, the ortho-II phase domains are prevalent. Nevertheless, the superconducting characteristics are strongly depressed, indicating that there are no superconducting phases localized at the intergrain regions. Oxygen diffusion slow processes occur in the sample when it is stored at room temperature, which increase the local order of the structure, confirming the ortho-II phase.

Acknowledgments

This work was supported by MURST under the project ‘Sviluppo di componentistica superconduttiva avanzata e sua applicazione a strumentazione biomedica’. One of the authors (ID) has been supported by INFM under the project ‘DEBUSSY’.

References

[1] Dam B, Huijbregste J M, Klaasen F C, Van der Geest R C F, Doornbos G, Rector J H, Testa A M, Freisem S, Martinez J C, Stauble-Pumpin B and Griessen R 1999 *Nature* **399** 439
[2] Mezzetti E, Chiodoni A, Gerbaldo R, Ghigo G, Gozzelino L, Minetti B, Camerlingo C and Giannini C 2001 *Eur. Phys. J.* B **19** 357
[3] Iliev M N, Zhang P X, Habermeier H-U and Cardona M 1997 *J. Alloys Compd.* **251** 99
[4] Garcia-Gonzàlez E, Wagner G, Reedyk M and Habermeier H-U 1995 *J. Appl. Phys.* **78** 353
[5] Huong P V 1991 *Physica* C **180** 128
[6] Liarokapis E 2000 *J. Supercond. (*incorporating *Novel Magnetism)* **13** 889
[7] Burns G, Dacol F H, Feild C and Holtzberg F 1990 *Solid State Commun.* **75** 893
[8] Fantini S, Ulivi L and Zoppi M 1995 *Solid State Commun.* **93** 519
[9] Burns G, Dacol F H, Feild C and Holtzberg F 1991 *Physica* C **181** 37
[10] Straube E, Holwein D and Kubanek F 1998 *Physica* C **295** 1